Dual Transduction Signaling by a *Xenopus* Muscarinic Receptor:
Adenylyl Cyclase Inhibition and MAP Kinase Activation

Luisa Herrera,[2] María Victoria Hinrichs,[2] Jorge Frías,[2] Silvio Gutkind,[1] and Juan Olate[2]*

[1]Molecular Signaling Unit, Laboratory of Cellular Development and Oncology, National Institute of Dental Research, National Institutes of Health, Bethesda, Maryland
[2]Laboratorio de Genética Molecular, Departamento de Fisiopatología, Facultad de Ciencias Biológicas, Universidad de Concepción, Concepción, Chile

Abstract   Using transient transfection of COS-7 and human embryonic kidney 293 cells, we studied the functional properties of a previously cloned muscarinic *Xenopus* receptor [Herrera et al. (1994): FEBS Lett 352:175–179] and its coupling to adenylyl cyclase (AC) and mitogen-activated protein kinase (MAPK) pathways. Expression of the *Xenopus* muscarinic receptor results in the inhibition of AC activity and activation of the MAPK pathway through a mechanism that involves a *Pertussis*-toxin-sensitive G-protein and the G$\beta\gamma$ subunits. The signal transduction properties of this receptor are similar to the mammalian m2 and m4 muscarinic receptors. These results strongly support the idea that inhibition of AC and MAPK activation, signaled out from the muscarinic oocyte receptor, are involved in the oocyte maturation process. J. Cell. Biochem. 65:75–82.   © 1997 Wiley-Liss, Inc.

Key words: adenylyl cyclase; MAP kinase; G protein; $\beta\gamma$ subunit; *Xenopus* oocyte; signal transduction

The *Xenopus laevis* oocyte has been used widely to study the maturation process and cell division because it has a cell division cycle without interphase. Thus, frog oocytes offer a very good system to study different proteins involved in the regulation of the cell cycle. The induction of oocyte maturation involves an initial action of agonists at the oocyte surface. Anfibian stage VI oocytes are arrested in late G2 of meiosis I and must progress to the second meiotic metaphase before fertilization is possible. The induction of meiosis in vivo is triggered by progesterone action, which acts directly on the oocyte to initiate the process of maturation [Baulieu et al., 1978; Maller, 1983; Schuetz and Glad, 1985]. Two signal transduction systems have been implicated in the initiation of the maturation process in *Xenopus laevis* oocyte: the adenylyl cyclase (AC) and phospholipase C (PLC) [Maller, 1983; Cicirelli et al., 1988; Kroll et al., 1991]. Both enzymes are present in the plasma membrane of the oocyte and are sensitive to different ligands. Progesterone inhibits the AC activity by an unusual mechanism that causes maturation by lowering cytosolic cAMP levels [Olate et al., 1984; Sadler et al., 1984]. Interestingly, acetylcholine also inhibits oocyte AC by a still unknown mechanism [Sadler et al., 1984], thus potentiating progesterone action and accelerating the maturation process in time [Sadler et al., 1984]. Furthermore, electrophysiological studies in the oocyte have shown the presence of two types of muscarinic receptors, M3 and M1 [Davidson et al., 1991]. Activation of these receptors increases the cytosolic levels of inositol 1,4,5-trisphosphate (IP3) through the activation of PLC, which is probably mediated by a Go protein [Kroll et al., 1991; Blitzer et al., 1993]. IP3 causes release of cytosolic Ca^{++} from endogenous stores, which in turn causes the opening of Cl^- channels and membrane depolarization [Blitzer et al., 1993].

In mammals, m1 and m3 mAchR subtype receptors are coupled with PLC activation and m2 and m4 with AC inhibition [Felder, 1995; Peralta et al., 1987]. Furthermore, m2 and m4 receptors in some cells also activate the mitogen-activated protein kinase (MAPK) pathway and regulate the cell cycle progress [Crespo et al., 1994]. The cell cycle resumption in *Xenopus* oocytes is accompanied by the activation of different kinases, which can serve as biochemical markers of meiotic maturation. Several inducers of oocyte maturation can activate a pre-existing factor, the pre–maturation-promoting factor (pre-MPF). Activation of pre-MPF induces activation of the cell cycle, and as a consequence there is a burst in phosphorylation of intracellular substrates 30–60 min before the breakdown of the germinal vesicle (GVBD). One intracellular subtrate is the MAPK, which is activated during M-phase transition, and constitutes part of the kinase cascade downstream of the MPF activation. The meiotic maturation process clearly depends on MAPK activation [Ferrel et al., 1991; Kosako et al., 1994]. These findings suggest the presence in *Xenopus* oocytes of two different signal transduction systems that are sensitive to acetylcholine: AC, and MAPK both involved in oocyte maturation.

In this context, we cloned a *Xenopus laevis* oocyte muscarinic receptor (XlmR) of the m4 subtype that could be mediating the inhibition of AC and MAPK activation in the oocyte [Herrera et al., 1994]. To test this hypothesis, we took the advantage of the functional coupling of exogenous receptors to endogenous signal transduction systems in cultured cells to study the binding and coupling properties of XlmR to AC and MAPK pathways by transient expression of the receptor in COS-7 and human embryonic kidney (HEK)-293 cells. In this report, we show that XlmR inhibits AC with a *Pertussis*-toxin (PTX)-sensitive Gα protein and activates the MAPK pathway with the G$\beta\gamma$ dimer, thus more closely resembling the m2 and m4 mammalian-type receptors and confirming our previous XlmR classification as an m4 type.

MATERIALS AND METHODS
Cells and Transfection

HEK-293 and COS-7 cells were grown in Dulbecco's modified Eagle's medium (DMEM), supplemented with 10% inactivated fetal calf serum, 100 IU/ml penicillin, and 100 μg/ml streptomycin. Cells were incubated in a humidified incubator containing 5% CO_2 at 37°C until 80% of confluence was reached. Transfections were performed by using calcium phosphate for HEK-293 cells, DEAE-dextran/chloroquine for COS-7 cells, and 5 μg of DNA from each plasmid.

cDNAs and Plasmids

Complementary DNA coding for the full-length XlmR was subcloned into the pcDNA3B plasmid as follows. The DNA region containing the Kozak sequence was subcloned into the pGEM15Zf(−) plasmid (Promega). The XlmR cDNA was then excised from the pAGA2 plasmid and subcloned into the pGEM15Zf(−)/Kozak plasmid. The DNA region containing tha Kozak and XlmR cDNAs was subcloned into the pcDNA3B plasmid to generate the pcDNA3B/XlmR construction. Plasmid pcDNA1 containing the human dopamine D1 receptor, human transducin Gαt, and MAPK, plasmid pCMV containing the human m1 muscarinic receptor, and Okayama Berg plasmid containing the human m2 muscarinic receptor were kindly donated by Silvio Gutkind (Molecular Signaling Unit, Laboratory of Cellular Development and Oncology, National Institute of Dental Research, National Institutes of Health, Bethesda, MD).

Radioligand Binding

COS-7 cells transfected with the pcDNA3B/XlmR plasmid were harvested after 48 h of incubation and homogenized in binding buffer (20 mM Tris, pH 7.4, 100 mM NaCl, and 5 mM $MgCl_2$) using a high speed homogenizer. A cell membrane fraction (pellet) was prepared by centrifugation at 27,000g for 15 min. For the saturation experiments, each tube contained 50 μg of membrane, 200 pM of [³H]-N-methyl-scopolamine ([³H]NMS), and the indicated cold NMS concentrations for a final volume of 1 ml. Competition binding experiments were done under similar conditions in the presence of the corresponding competitor at the indicated concentrations for a final volume of 1 ml. The bound radiolabeled ligand was collected by filtration on Whatman GF/C filters. These filters were then rapidly washed three times with ice-cold binding buffer, and the associated radioactivity was determined. The dissociation constants for [³H]NMS were calculated by using the data from saturation experiments. The K_i constants values for methoctramine, 4-DAMP, and pirenzepine were calculated by using the data from the competition experiments and corrected for the Cheng–Prusoff shift. Nonspecific

binding was determined by using 10^{-6} M of atropine.

Phosphoinositide Turnover

Phosphoinositide turnover studies were performed as described by Crespo et al. [1994]. Following 24 h of transfection, 1 ml of transfected cells was seeded into 24-well plates and labeled with 1 µCi/well of [3H]myo-D-inositol for 24 h. Cells were washed with prewarmed serum-free DMEM, incubated in the same medium containing 10 mM LiCl for another 4 h, and then incubated with the agonists for another 30 min. Cells were then lysed with 1 ml of cold 5% trichloroacetic acid and neutralized, and 800 µl of the neutralized fraction were added to 1-ml Dowex AG-1X8 (BIORAD) columns. After washing three times with 5 ml of water, the total inositol phosphates (IPs) were eluted with 10 ml of 0.2 M ammonium formate/ 0.1 M formic acid. Radioactivity was determined by liquid scintillation counting.

cAMP Assay

cAMP levels were determined essentially as described by Stephens et al. [1993]. After 24 h of transfection, 1 ml of transfected cells was seeded into a 24-well plate. Intact attached monolayer cells were washed with serum-free DMEM medium and incubated in the same medium containing 1 mM isobutil-1-methyl-xantine for 30 min. Cells were then incubated for 20 min in the presence of the ligands, and the reaction was stopped by adding 100 µl of 0.1 M HCl. Scrapped cells were centrifuged at 4°C for 5 min, and the supernatant was collected and assayed for cAMP content with a competitive protein binding assay kit (Amersham). To analyze the PTX effect, transfected cells were preincubated for 18 h with 20 ng/ml of the toxin.

MAPK Activity

MAPK activation was determined essentially as described by Crespo et al. [1994]. Transfected COS-7 cells were starved overnight, incubated with the indicated ligands for 5 min, lysed, and MAPK immunoprecipitated with 2 µg of the antihemmaglutinin epitope antibody 12CA5. MAPK activity was measured in the immunoprecipitates in an appropiate reaction buffer containing 1 µCi [γ-32P]ATP and myelin basic protein (MBP) as substrates. Phosphorylated MBP was visualized by PAGE-SDS (poly-acrylamide gel electrophoresis in the presence of sodium dodecyl sulfate) and autoradiography. To analyze the PTX effect, transfected cells were preincubated for 18 h with 20 ng/ml of the toxin.

Data Analysis

[3H]NMS K_d and B_{max} values were derived using Scatchard analysis [Scatchard, 1949]. K_i, K_{50}, and fit analysis of agonist binding curves were calculated using the computer program INPLOT (GraphPAD Software, San Diego, CA), and K_i values were corrected for the Cheng–Prusoff shift. To determine whether the mean of the experiments differed significantly, a paired t-test (Student's t-test) was applied, and P values were obtained.

RESULTS

Ligand Binding Characteristics of XlmR

To establish whether the cloned *Xenopus* receptor is indeed a muscarinic receptor, COS-7 cells were transfected with the recombinant plasmid pcDNA3B/XlmR. Membranes were then prepared from these transfected cells and assayed for their ability to bind specifically the muscarinic antagonist [3H]NMS and displace with the selective antagonists pirenzepine, 4-DAMP, and methoctramine. Other nonrelated muscarinic ligands were also used to test binding specificity. Figure 1A shows the result of the saturation analysis carried out with increasing concentrations of [3H]NMS in the absence and presence of 1 µM atropine. Figure 1B shows the linear relationship obtained by replotting the equilibrium binding data according to Scatchard [1949]. The estimated K_d for [3H]NMS binding was 1 nM ± 0.045 (mean ± S.D., n = 3). Equilibrium displacement studies were carried out with the muscarinic antagonists pirenzepine (selective for M1), 4-DAMP (selective for M3), and methoctramine (selective for M2). Figure 2 shows the binding inhibition curves obtained with these antagonists, with calculated K_i values of 5 nM for DAMP, 0.1 µM for pirenzepine, and 0.7 µM for methoctramine (n = 3). Control cells, transfected with the nonrecombinant vector, did not show any binding activity (data not shown).

Coupling of XlmR to AC and PLC

To determine to which effector system XlmR was coupled, we investigated the effect of carbachol on both phosphoinositide hydrolysis and
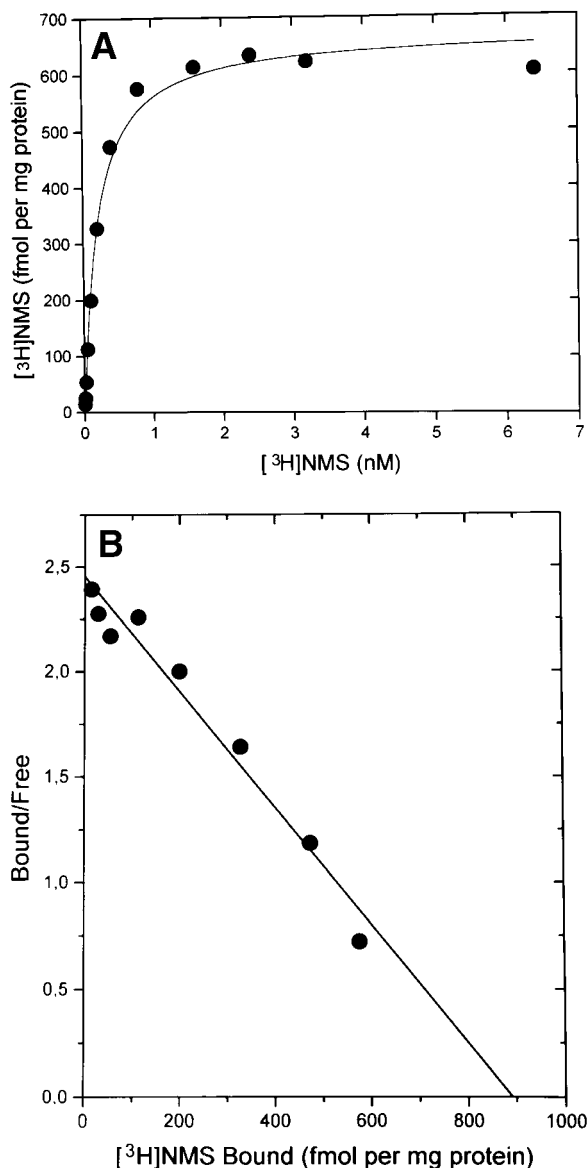
Fig. 1. Saturation (**A**) and Scatchard (**B**) binding analyses of [³H]NMS in COS-7 cells transiently expressing XlmR. Fifty micrograms of COS-7 cell membrane were incubated for 1 h with different concentrations of [³H]NMS in the presence or absence of 1 μM atropine. Assays were performed in triplicate, and the mean values are plotted.

Fig. 2. Displacement of [³H]NMS binding by various antagonists in COS-7 cells transiently expressing XlmR. Fifty micrograms of COS-7 cell membrane were incubated for 1 h with 200 pM of [³H]NMS in the presence of increasing concentrations of unlabeled DAMP, pirenzepine, and methoctramine. Assays were done in triplicate.

AC production. Experimental conditions were selected to optimize the response of AC and PLC to carbachol in XlmR-transfected COS-7 cells. The same procedure was done for the experiments performed in HEK-293 cells (data nor shown). Carbachol-induced inhibition of AC was determined by measuring intracellular cAMP levels after phenoldopamine stimulation (synthetic dopamine antagonist) of a coexpressed human dopamine D1 receptor. Phe-
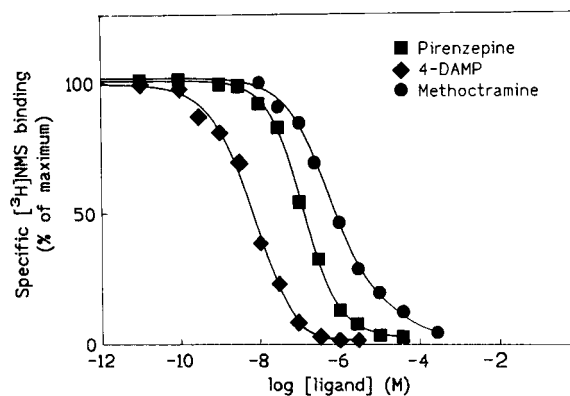
noldopamine-stimulated AC activity was inhibited by nearly 40% by carbachol in COS-7 cells expressing the human m2 receptor ($P = 5 \times 10^{-5}$) or the XlmR ($P = 1.5 \times 10^{-6}$) (Fig. 3). Atropine, a muscarinic antagonist, reverted the carbachol-dependent inhibition and restored the cAMP levels to those initially obtained with the phenoldopamine treatment. COS-7 cells, transfected with the dopamine D1 receptor alone, did not show any carbachol effect. These results clearly show that XlmR behaves like the mammalian m2 muscarinic receptor by coupling to AC inhibition. Carbachol stimulated the accumulation of total IP in cells transfected with the human m1 receptor, and atropine blocked this stimulation (Fig. 4). In contrast, in cells transfected with the human m2 receptor or XlmR, no effect on IP levels was seen with carbachol and atropine. These results clearly show that XlmrR does not couple to the PLC pathway as the mammalian m1 and m3 receptors do.

Activation of MAPK by XlmR

To investigate the coupling of XlmR to the MAPK pathway, we coexpressed XlmR in COS-7 cells with an MAPK enzyme tagged with a hemmaglutinin epitope (HA-MAPK). Figure 5 shows MAPK activation kinetic analysis induced by carbachol. Maximum MAPK activation was obtained 5 min after adding the ligand. As a control, in nontransfected COS-7 cells, epidermal growth factor (EGF), an activator of this pathway, caused activation of the MAPK with its endogenous receptor. Treat-
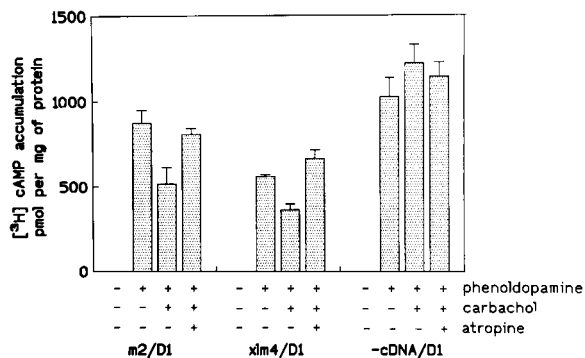
Fig. 3. cAMP response in COS-7 cells transfected with XlmR and carbachol and atropine effects on phenoldopamine-stimulated cAMP accumulation. Values for each treatment are the means ± S.E. of six determinations from two separate experiments. m2/D1, cells cotransfected with the human m2 and dopamine D1 receptors; xlm4/D1, cells cotransfected with XlmR and human dopamine D1 receptor; −cDNA/D1, cells transfected only with the human D1 dopamine receptor; +, addition; −, no addition. To determine whether the mean of the six experiments were significant, a paired t-test was applied; P values were significant for m2/D1 (5×10^{-5}) and xlm4/D1 (1.5×10^{-6}) carbachol inhibitions.
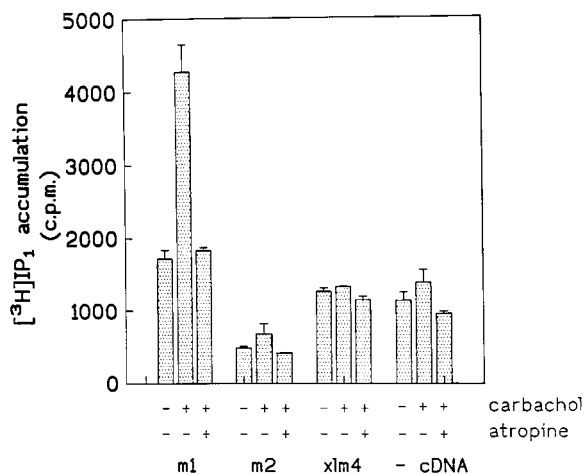

Fig. 4. Effects of carbachol and atropine on phosphoinositide breakdown in COS-7 cells transiently transfected with human m1 and m2 receptors and XlmR. m1, cells transfected with the human m1 receptor; m2, cells transfected with the human m2 receptor; xlm4, cells transfected with XlmR; −cDNA, untransfected cells; +, addition; −, no addition.

ment with PTX, which uncouples certain types of G-protein by ADP ribosylation, nearly abolished MAPK activation by human m2 and XlmR but not by human m1 or EGF receptors (Fig. 6). These experiments clearly show that MAPK is being activated by XlmR with a PTX-sensitive G-protein, presumably a member of the Gi family. To investigate whether the Gβγ dimer could participate in the activation of the MAPK, we

overexpressed the transducin Gαt subunit. Expression of Gαt did not affect the activation of MAPK by EGF but blocked its activation by m1, m2 and XlmR (Fig. 7), indicating that Gβγ dimers are involved in the signaling from the *Xenopus* G-protein-coupled receptor to MAPK.

DISCUSSION

Cell cultured clones expressing recombinant, homogeneous populations of G-protein-coupled receptors represent a useful model for studying agonist binding and coupling to particular signal transduction pathways [Hossey, 1992]. By expressing an XlmR in COS-7 and HEK-293 cells, it was possible to study its pharmacological and functional properties. Membranes from nontransfected COS-7 cells display no [3H]NMS binding (data not shown), but those from transfected cells exhibit a specific and saturable [3H]NMS binding. The competitive inhibition binding curves show that this receptor presents similar affinities for DAMP (M2 = 7–10 nM) and pirenzepine (M1 = 0.08 μM, M2 = 0.138 μM) but lower affinity for methoctramine (M2 = 4 nM) as compared with published values [Hulme et al., 1990]. The displacement curves for XlmR were more similar to that observed for the expressed hm2R receptor than for the hm1R receptor (data not shown). A more complete antagonist profile will be necessary to define a unique pharmacological binding pattern for this receptor. These differences could be due to the XlmR amino acid sequence, specifically to the extracellular and cytosolic loops, where the most significant differences in amino acid composition have been described [Herrera et al., 1994]. Based on deduced amino acid sequence comparison studies, we previously defined XlmR as an m4 subtype [Herrera et al., 1994], but the competition binding experiments do not allow us to confirm this notion, indicating that additional studies will be necessary to determine a unique antagonist/agonist binding pattern.

The dopamine-dependent increase of cAMP levels in COS-7 cells were reduced by nearly 40% ($P = 1.5 \times 10^{-6}$) by the muscarinic agonist carbachol, indicating that XlmR is coupled with AC inhibition. The inhibition was completely abolished by the antagonist atropine, suggesting the muscarinic specificity on this effect. Similar results were observed when the human m2 receptor coupling properties were analyzed, and no effect on AC activity was found with the human m1 receptor. The observed alteration in
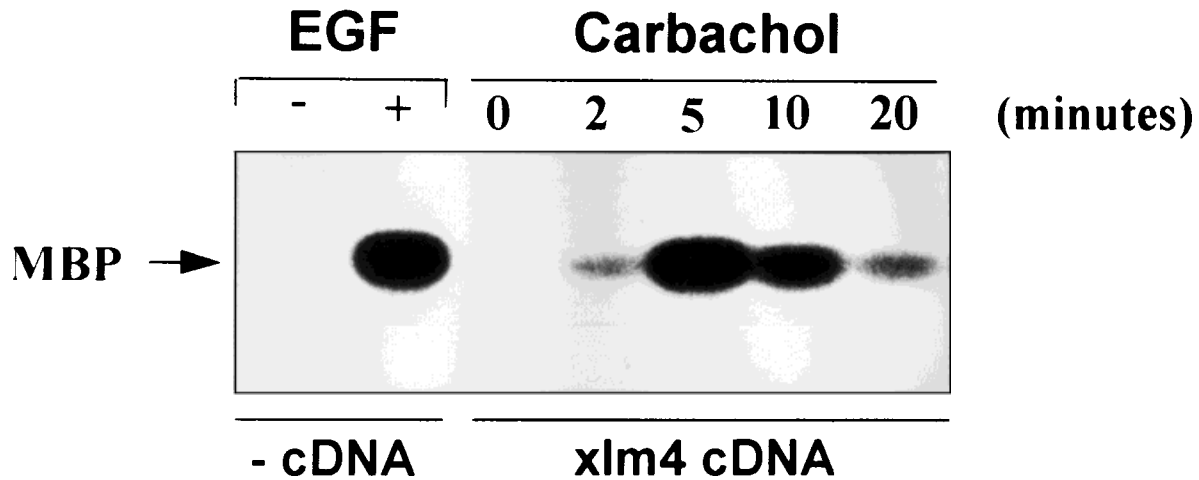
Fig. 5. Effect of carbachol on MAPK activation in COS-7 cells cotransfected with an epitope-tagged MAPK and XlmR. MBP, electrophoretic mobility of the phosphorylated substrate myelin basic protein; xlm4, cells transfected with XlmR; −cDNA, untransfected cells; +, addition; −, no addition. Numbers on top denote time (min).
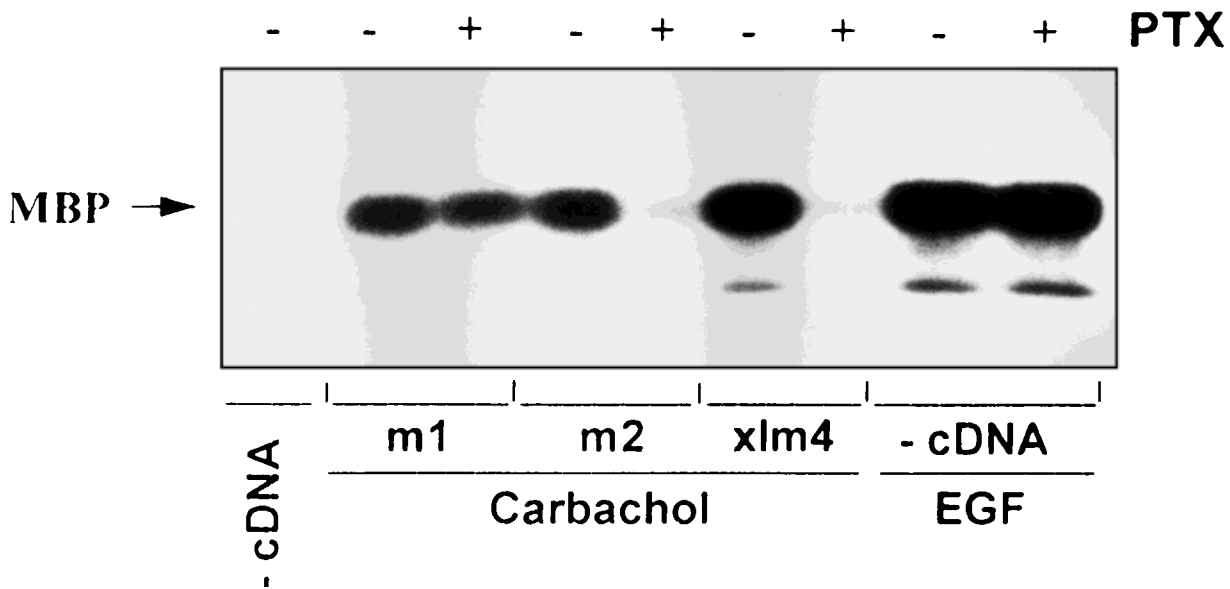

Fig. 6. Effect of *Pertussis* toxin (PTX) on carbachol and epidermal growth factor (EGF)-induced MAPK activation in COS-7 cells cotransfected with an epitope-tagged MAPK, the human m1 and m2 receptors, and XlmR. MBP, electrophoretic mobility of the phosphorylated substrate myelin basic protein; m1, cells transfected with human m1 receptor; m2, cells transfected with human m2 receptor; xlm4, cells transfected with XlmR; −cDNA, untransfected cells; +, addition; −, no addition.

cAMP levels was not due to changes in the cAMP phosphodiesterase enzymatic activity because the inhibitor IMBX was present in the assay mixture. The carbachol-induced phosphoinositide breakdown was observed only in cells transfected with the human m1 receptor and not in cells expressing the XlmR or human m2 receptor. These results are in agreement with previous findings that show that mammalian m2 and m4 receptors are coupled preferently with AC inhibition and m1 and m3 receptors

with PLC activation [Felder, 1995]. Based on these findings, we conclude that the signal transduction properties of XlmR, heterologously expressed in COS-7 cells, are the same as those expected for the m2 and m4 subtypes, thus supporting the sequence homology found between XlmR and human m4 receptor [Herrera et al., 1994].

Activation of MAPK by carbachol only occurs in XlmR-transfected COS-7 cells and not in control cells (data not shown), where MAPK
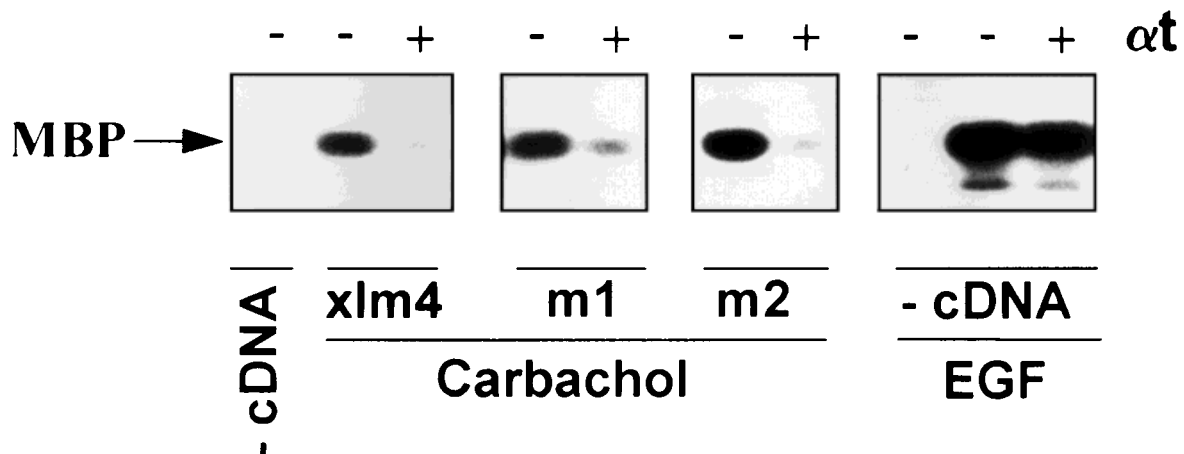
Fig. 7. Effect of transducin Gαt on carbachol and epidermal growth factor (EGF)-induced MAPK activation in COS-7 cells cotransfected with an epitope-tagged MAPK, the human m1 and m2 receptors, and XlmR. MBP, electrophoretic mobility of the phosphorylated substrate myelin basic protein; αt, the alpha subunit of transducin; m1, cells transfected with the human m1 receptor; m2, cells transfected with the human m2 receptor; xlm4, cells transfected with XlmR; −cDNA, untransfected cells; +, addition; −, no addition.

activation is only induced by the endogenous EGF receptor. Our findings clearly indicate that carbachol-induced MAPK activation is initiated by the expressed XlmR. The involvement of a G-protein in this MAPK activation was demonstrated by pretreating transfected cells with PTX and then challenging them with the carbachol action. The coupling to AC inhibition also involves a G-protein, probably a Gi type, because PTX abolishes carbachol action (data not shown). The presence of a Gi-type protein in *Xenopus* oocytes has been demonstrated [Goodhardt et al., 1984; Olate et al., 1984, 1985]. Overexpression of Gαt blocked carbachol-induced MAPK activation in cells transfected with the human m1 and m2 receptors and XlmR but it did not modify EGF-induced stimulation, indicating the participation of the Gβγ dimer in MAPK activation. Expression of proteins that interact with the Gβγ dimer, e.g., β-adrenergic receptor kinase and transducin Gαt, decrease the free Gβγ intracellular levels, thus blocking Gβγ-dependent pathways such as raf-1 and MAPK activation [Crespo et al., 1994]. Our results are in good agreement with these findings, indicating that XlmR activates the MAPK pathway with a Gβγ-dependent mechanism. A similar mechanism may take place in the *Xenopus* oocyte, where the potentiation of oocyte maturation by acetylcholine reflects the activation of the MAPK pathway [Muslin et al., 1993; Yashar et al., 1993; Kosako et al., 1994], probably with XlmR.

REFERENCES

Baulieu E-E, Godeau F, Schorderet M, Schorderet-Slatkine S (1978): Steroid-induced meiotic division in *Xenopus laevis* oocytes: Surface and calcium. Nature (Lond) 275: 593–598.

Blitzer D, Omri G, DeVivo M, Carty D, Premont R, Codina J, Birnbaumer L, Cotecchia S, Caron M, Leftkowitz R, Landau E, Iyengar R (1993): Coupling of the expressed α_{1B}-adrenergic receptor to the phospholipase C pathway in *Xenopus* oocytes. J Biol Chem 268:7532–7537.

Cicirelli MF, Pelech SL, Krebs EG (1988): Activation of multiple protein kinases during the burst in protein phosphorylation that precedes the first meiotic cell division in *Xenupus* oocytes. J Biol Chem 263:2009–2019.

Crespo P, Xu N, Simonds W, Gutkind S (1994): Ras-dependent activation of MAP kinase pathway mediated by G-protein βγ subunits. Nature (Lond) 369:418–420.

Davidson A, Mengod G, Matus-Leibovich N, Oron Y (1991): Native *xenopus* oocytes express two types of muscarinic receptors. FEBS Lett 284:252–256.

Goodhardt M, Ferry N, Buscaglia M, Baulieu E-E, Hanoune J (1984): Does the guanine nucleotide regulatory protein Ni mediate progesterone inhibition of Xenopus oocyte adenylate cyclase? EMBO J 3:2653–2658.

Felder CC (1995): Muscarinic acetylcholine receptors: Signal transduction through multiple effectors. FASEB J 9:619–625.

Ferrel J, Wu M, Gerhart J, Martin G (1991): Cell cycle tyrosine phosphorylation of p34cdc2 and a microtubule-associated protein kinase homolog in xenopus oocytes and eggs. Mol Cell Biol 11:1965–1971.

Herrera L, Carvallo P, Antonelli M, Olate J (1994): Cloning of a *Xenopus laevis* muscarinic receptor encoded by an intronless gene. FEBS Lett 352:175–179.

Hossey MM (1992): Diversity of structure, signaling and regulation within the family of muscarinic cholinergic receptors. FASEB J 6:845–852.

Hulme E, Birdsall N, Buckley N (1990): Muscarinic receptor subtypes. Annu Rev Pharmacol Toxicol 30:633–673.

Kosako H, Gotoh Y, Nishida E (1994): Regulation and function of the MAP kinase cascade in *Xenopus* oocytes. J Cell Sci 18(Suppl):115–119.

Kroll S, Omri G, Landau E, Iyengar R (1991): Activated α subunit of Go protein induces oocyte maturation. Proc Natl Acad Sci USA 88:5182–5186.

Maller JL (1983): Interaction of steroids with the cyclic nucleotide system in amphibian oocytes. Adv Cyclic Nucl Res 15:295–298.

Muslin AJ, MacNicol AM, Williams LT (1993): Raf-1 protein kinase is important for progesterone-induced *Xenopus* oocyte maturation and acts downstream of mos. Mol Cell Biol 13:4197–4202.

Olate J, Allende C, Allende JE, Sekura R, Birnbaumer L (1984): Oocyte adenylyl cyclase Ni, yet the guanine nucle-otide-dependent inhibition by progesterone is not sensitive to pertussis toxin. FEBS Lett 175:25–29.

Olate J, Anker R, Allende JE (1985): Trearment of oocyte membrane with 2',3'-dialdehyde of guanosine triphosphate reduces progesterone inhibition of adenylyl cyclase. FEBS Lett 185–170.

Peralta E, Ashkenazi J, Winslow D, Smith J, Ramachandran J, Capon D (1987): Distinct primary structure, ligand-binding properties and tissue-specific expression of four human muscarinic acetylcholine receptors. EMBO J 6:3923–3927.

Sadler S, Maller J, Cooper D (1984): Progesterone inhibition of *Xenopus* oocyte adenylate cyclase is not mediated via the *Bordetella pertussis* toxin substrate. Mol Pharmacol 26:526–531.

Scatchard G (1949): The attraction of proteins for small molecules and ions. Ann NY Acad Sci 51:660–675.

Schuetz AW, Glad R (1985): *In vitro* production of meiosis inducing substance (MIS) by isolated amphibian (*Rana Pipiens*) follicle cells. Dev Growth Diff 27:201–205.

Stephens E, Kalinec G, Brann M, Gutkind S (1993): Transforming G protein-coupled receptors transduce potent mitogenic signals in NIH 3T3 cells independent on cAMP inhibition or conventional protein kinase C. Oncogene 8:19–22.

Yashar BM, Kelley C, Yee K, Errede B, Zon LI (1993): Novel members of the mitogen-activated protein kinase activator family in *Xenopus laevis*. Mol Cell Biol 13:5738–5748.